

Validity of the shape-independent approximation for Bose-Einstein condensates

B. D. Esry

ITAMP, Harvard-Smithsonian Center for Astrophysics, Cambridge, Massachusetts 02138

Chris H. Greene

Department of Physics and JILA, University of Colorado, Boulder, Colorado 80309-0440

(Received 14 September 1998)

The validity of the shape-independent approximation is studied for three trapped atoms. By comparing the total ground-state energy calculated using pseudopotentials in the Hartree-Fock approximation to the exact ground-state energy, the shape-independent approximation is shown to agree quantitatively only in the low-density limit. It is also shown using configuration interaction that a Dirac δ function is not suitable as a replacement for the two-body interaction in exact theories. [S1050-2947(99)01208-1]

PACS number(s): 03.75.Fi, 34.20.-b, 03.65.Nk

I. INTRODUCTION

The calculation of observables for current dilute atomic Bose-Einstein condensation (BEC) experiments is greatly simplified by the disparity in the length scales of the atomic interactions and the trapping potential. The s -wave scattering length a_{sc} characterizes the scale of atom-atom interactions and has a typical magnitude in the vicinity of 10–100 a.u. for alkali-metal atoms. The trap length scale is approximately the classical turning point of a single atom in the lowest oscillator state, and is typically on the order of a few microns in present experiments. The de Broglie wavelength associated with atomic motion in the nodeless condensate ground state is thus three to four orders of magnitude larger than the interaction length scale. The atom-atom interaction potential is consequently well-described in the shape-independent approximation (SIA), also referred to as the pseudopotential approximation. In using just the s -wave scattering length, it is also assumed that since the average interparticle spacing is much larger than a_{sc} , the effects of other particles can be neglected in obtaining the effective two-body interaction. The criterion for the validity of this assumption in the homogeneous case is typically written as $na_{sc}^3 \ll 1$, where n is the number density. This same condition has been applied to trapped atoms, taking n to be some characteristic number density in the trap. The precise nature of these assumptions for trapped gases was recently explored in detail by Proukakis *et al.* [1] using many-body perturbation theory. They obtained the validity condition for harmonically trapped atoms, $n4\pi\hbar^2 a_{sc}/m \ll \hbar\omega$.

In this paper, we develop an approach complementary to that of Proukakis *et al.* We compare the Hartree-Fock solution to a nearly exact solution of the Schrödinger equation for three atoms in a trap. We compare the total energy of the ground state in the two approaches over a broad range of trapping frequencies. As the frequency is varied, the density dependence of the SIA can be studied while keeping the number of atoms fixed. In fact, since mean-field theory depends only on the combination $Na_{sc}\sqrt{\omega}$, one can imagine that in some sense the number of atoms in the mean-field equation is being varied instead of the frequency. We will also demonstrate that the pseudopotential should be used directly in the Hamiltonian only with the understanding that

the Schrödinger equation *must not be solved exactly*—a point made below in several contexts. The ground-state energy calculated using configuration interaction, for instance, does not converge. We interpret this failure as a reflection of the pathological singularity of the three-dimensional Dirac δ function when used directly as a potential in the Schrödinger equation.

The shape-independent approximation amounts to replacing the atom-atom interaction potential by a δ function—the pseudopotential—whose strength is chosen so that the two-body scattering wave function is “reproduced asymptotically” in some sense. For the very-low-energy collisions taking place in the condensate, the coefficient of the δ function is simply proportional to the s -wave scattering length. Corrections for higher energies and higher partial waves can also be made [2,3]. The s -wave pseudopotential approximation can be viewed loosely as a replacement of the physical atom-atom interaction by a hard sphere whose radius equals the scattering length. One of the first instances in which the shape-independent approximation was employed in this spirit was in a 1935 article by Fermi [4]. He introduced (in effect) the contact potential and used it to obtain a simple formula for the energy levels of a Rydberg atom in the presence of a neutral perturbing rare-gas atom. In the context of a weakly interacting gas, the pseudopotential was first used by Huang [2] to derive the low-lying energy spectrum for bosons in the perturbative limit.

A road map of the present study is as follows. Section II details the various theoretical approaches used in this work, namely the hyperspherical, Hartree-Fock, and configuration interaction approaches. Section III compares the ground-state energies obtained in each approximation and discusses the implications for the use of the pseudopotential in BEC theory. We also present numerical evidence for the failure of the pseudopotential as an “exact” interaction potential by documenting the divergence of the ground-state energy within the configuration interaction approach. Section IV summarizes our conclusions based on these results.

II. THEORY

There are two general approaches to solving the many-body Schrödinger equation: treating the particles collectively

and treating the particles independently. Currently, for two- and three-electron systems, the former approach—the Hylleraas expansion in particular—provides the most accurate bound-state energies available. Another collective coordinate approach, the hyperspherical coordinate method, has proven useful in describing multiple excitations in two- and three-electron systems, in describing weakly bound systems such as the helium trimer, and in describing the two-electron continuum in double ionization. For more than a few particles, however, such approaches become intractable and the simplifying independent-particle approximation must be made. The successes of this approach are also well known and range from atomic structure to the current application to a system of trapped bosonic atoms. Configuration interaction (CI) is one way to include correlations beyond the independent-particle approximation. For the ground state of three particles, all of these methods remain of manageable size. We briefly describe the hyperspherical, Hartree-Fock, and configuration interaction approaches and their specialization to the trapped boson problem in the next three sections.

A. Adiabatic hyperspherical method

The adiabatic hyperspherical method has been explained in detail in several previous works [5–8]. Here, we outline the method and the necessary modifications for three identical, interacting particles in an isotropic harmonic trapping potential.

The Schrödinger equation in laboratory frame coordinates $(\mathbf{r}_1, \mathbf{r}_2, \mathbf{r}_3)$ is given by

$$\left[\sum_{i=1}^3 -\frac{\hbar^2}{2m} \nabla_{\mathbf{r}_i}^2 + \frac{1}{2} m \omega^2 r_i^2 + \sum_{i<j}^3 V(r_{ij}) \right] \Psi = E \Psi, \quad (1)$$

assuming the particles interact *via* the two-body potential $V(r)$. In this equation, m is the mass of the particles and ω is the frequency of the trap. In principle, for three interacting atoms there are also pure three-body terms due to the composite nature of the atoms. The lowest such term appearing in perturbation theory was found by Axilrod and Teller [9] (see also Ref. [10]) and is essentially the three-body analog of the van der Waal's interaction. This Axilrod-Teller interaction depends on the hyperradius as R^{-9} asymptotically, however, so we neglect it here and in the Hartree-Fock equations.

Equation (1) can be transformed to the coordinates of the center of mass \mathbf{X} plus Jacobi coordinates $\boldsymbol{\rho}_1$ and $\boldsymbol{\rho}_2$ for the internal motion:

$$\mathbf{X} = \frac{1}{3}(\mathbf{r}_1 + \mathbf{r}_2 + \mathbf{r}_3),$$

$$\boldsymbol{\rho}_1 = \mathbf{r}_2 - \mathbf{r}_1, \quad \boldsymbol{\rho}_2 = \mathbf{r}_3 - \frac{1}{2}(\mathbf{r}_2 + \mathbf{r}_1).$$

The advantage of Jacobi coordinates is that they maintain the simple form of the kinetic energy operator, while also decoupling the center of mass and the relative motion in the case of a harmonic (or vanishing) external field. In terms of $(\mathbf{X}, \boldsymbol{\rho}_1, \boldsymbol{\rho}_2)$, the Schrödinger equation is thus written

$$[H_{\text{CM}} + H_{\boldsymbol{\rho}_1} + H_{\boldsymbol{\rho}_2} + V_{\text{tot}}(\boldsymbol{\rho}_1, \boldsymbol{\rho}_2)] \Psi = E \Psi.$$

The individual oscillator Hamiltonians in these coordinates are

$$H_{\text{CM}} = -\frac{\hbar^2}{2M} \nabla_{\text{CM}}^2 + \frac{1}{2} M \omega^2 X^2,$$

$$H_{\boldsymbol{\rho}_1} = -\frac{\hbar^2}{2\mu_1} \nabla_{\boldsymbol{\rho}_1}^2 + \frac{1}{2} \mu_1 \omega^2 \rho_1^2,$$

$$H_{\boldsymbol{\rho}_2} = -\frac{\hbar^2}{2\mu_2} \nabla_{\boldsymbol{\rho}_2}^2 + \frac{1}{2} \mu_2 \omega^2 \rho_2^2,$$

with $M = 3m$, $\mu_1 = m/2$, and $\mu_2 = 2m/3$. The interaction $V_{\text{tot}}(\boldsymbol{\rho}_1, \boldsymbol{\rho}_2)$ is the pairwise sum of two-body interactions from Eq. (1) and depends only on the internal coordinates. The center-of-mass motion can thus be separated from the internal motion by writing the wave function as $\Psi(\mathbf{X}, \boldsymbol{\rho}_1, \boldsymbol{\rho}_2) = \varphi(\mathbf{X}) \psi(\boldsymbol{\rho}_1, \boldsymbol{\rho}_2)$. The equation for the motion of the center of mass is then simply the harmonic-oscillator equation

$$H_{\text{CM}} \varphi_{nlm}(\mathbf{X}) = E_n \varphi_{nlm}(\mathbf{X}).$$

The energy eigenvalues are $E_n = (n + \frac{3}{2}) \hbar \omega$, and the eigenstates are the isotropic oscillator solutions.

Defining mass-weighted, body-frame hyperspherical coordinates [5] as

$$R^2 = \rho_1^2 + \frac{4}{3} \rho_2^2, \quad 0 \leq R < \infty,$$

$$\tan \phi = \frac{2}{\sqrt{3}} \frac{\rho_2}{\rho_1}, \quad 0 \leq \phi \leq \frac{\pi}{4},$$

and

$$\cos \theta = \frac{\boldsymbol{\rho}_1 \cdot \boldsymbol{\rho}_2}{\rho_1 \rho_2}, \quad 0 \leq \theta \leq \frac{\pi}{2},$$

the Schrödinger equation for the internal motion is

$$\left(-\frac{\hbar^2}{2\mu} \frac{\partial^2}{\partial R^2} + \frac{1}{2} \mu \omega^2 R^2 + H_{\text{ad}} \right) \psi(R, \phi, \theta) = \epsilon \psi(R, \phi, \theta), \quad (2)$$

where H_{ad} is the adiabatic Hamiltonian

$$H_{\text{ad}}(R; \phi, \theta) = \frac{\hbar^2}{2\mu R^2} \left(\Lambda^2 - \frac{1}{4} \right) + V_{\text{tot}}(R, \phi, \theta).$$

In the body-frame coordinates, the grand angular momentum operator Λ^2 is given by

$$\Lambda^2 = -\frac{\partial^2}{\partial \phi^2} - \frac{1}{\sin^2 \phi \cos^2 \phi \sin \theta} \frac{\partial}{\partial \theta} \left(\sin \theta \frac{\partial}{\partial \theta} \right).$$

Note that the wave function $\psi(R, \phi, \theta)$ is rescaled by the factor $R^{5/2} \sin \phi \cos \phi$ in order to eliminate first derivatives from the kinetic energy operator.

In the adiabatic approach, R is treated as a fixed parameter, and the equation

$$H_{\text{ad}}(R; \phi, \theta) \Phi_\nu(R; \phi, \theta) = U_\nu(R) \Phi_\nu(R; \phi, \theta) \quad (3)$$

solved for the adiabatic potentials $U_\nu(R)$ and channel functions $\Phi_\nu(R; \phi, \theta)$. The hyperradius is symmetric under all permutations of particles so that all of the identical particle symmetry must be accounted for in the channel functions. For spin-polarized indistinguishable bosons, Φ_ν must be completely symmetric under all permutations.

We solve Eq. (3) using basis splines [11]. Since the basis splines are localized, the resultant matrix, while large (on the order of thousands), is sparse—typically fewer than 20% of the entries are nonzero. These large sparse matrices can be diagonalized on workstations by using the `arpack` package (publicly available on the world wide web [12]) which is based upon a variant of the Lanczos algorithm [13]. This combination of techniques provides an efficient means to calculate the lowest eigenvalues and eigenvectors of the adiabatic equation, Eq. (3).

An exact solution to the Schrödinger equation can be constructed by expansion into the adiabatic channel functions:

$$\psi(R, \phi, \theta) = \sum_\nu F_\nu(R) \Phi_\nu(R; \phi, \theta),$$

which after substitution into Eq. (2) becomes a set of coupled hyperradial equations for the $F_\nu(R)$ that can be solved numerically. The channels are coupled through the dependent of Φ_ν on R . Neglecting the coupling between different channels, however, leads to a simple and useful set of single channel equations:

$$\left(-\frac{\hbar^2}{2\mu} \frac{d^2}{dR^2} + \frac{1}{2} \mu \omega^2 R^2 + U_\nu + W_{\nu\nu} \right) F_{\nu n} = E_{\nu n} F_{\nu n}, \quad (4)$$

where

$$W_{\nu\nu}(R) = -\frac{\hbar^2}{2\mu} \left\langle \Phi_\nu(R) \left| \frac{\partial^2}{\partial R^2} \right| \Phi_\nu(R) \right\rangle.$$

The quantum numbers ν and n label the channel and energy eigenstate within a channel, respectively. Equation (4) is a one-dimensional radial Schrödinger equation with an effective hyperradial potential $U_\nu(R) + W_{\nu\nu}(R)$ that determines the three-body spectrum in the adiabatic approximation. It can be shown [14] that the ground-state energy obtained by solving Eq. (4) is an upper bound to the true ground-state energy. This can be simply understood from the fact that this approach is formally equivalent to applying the Rayleigh-Ritz variational principle, using a trial wave function of the form

$$\psi'_{\nu n}(R, \phi, \theta) = F_{\nu n}(R) \Phi_\nu(R; \phi, \theta).$$

The variational principle then guarantees that the energy thus obtained is an upper bound to the true ground-state energy.

Dropping $W_{\nu\nu}(R)$ from Eq. (4) gives the useful result that the energy obtained is a lower bound to the exact ground-state energy [14]. This corresponds to the familiar Born-Oppenheimer approximation. The energy calculated variationally, however, is often much closer to the actual energy than is the lower bound.

As a ‘‘realistic’’ interaction potential in Eq. (1), we have chosen the Morse potential [15,16],

$$V(r) = D e^{-\alpha(r-r_0)} (e^{-\alpha(r-r_0)} - 2). \quad (5)$$

The constants D , α , and r_0 are chosen to set the dissociation limit, width of the potential well, and location of the well minimum, respectively. The only significant difference from a real neutral atom-atom interaction is the absence of van der Waal’s r^{-6} tail. This poses no serious difficulty since both can be considered short-range interactions for the purposes of (*s*-wave) scattering calculations and since we consider physics that is controlled essentially by only the scattering length. We have fixed the constants α and r_0 in the Morse potential to be $\alpha = 0.35$ a.u. $^{-1}$ and $r_0 = 11.65$ a.u., which approximate the Rb+Rb triplet interaction potential [17]. The constant D has been left free to vary in order to generate different scattering lengths.

The large difference in length scales that makes the pseudopotential so useful in mean-field calculations leads to difficulties in an exact calculation such as the hyperspherical approach. For example, the classical turning point is at approximately 17 700 a.u. in an isotropic trap with a frequency of 133 Hz. It is both difficult and unnecessary to calculate the potential curves numerically to such a large distance. The difficulty lies in the fact that the two-body interaction region in the (ϕ, θ) plane shrinks roughly as R^{-1} so that the numerical solution of the adiabatic eigenvalue equation becomes increasingly intensive numerically as R increases. But, for the hyperradial potential that correlates to three free atoms at $R \rightarrow \infty$, the asymptotic form of the potential for short range two-body interactions is known [18] to be

$$U_0(R) \rightarrow \frac{15}{8\mu R^2} + \frac{\alpha a_{\text{sc}}}{R^3} + \frac{\beta a_{\text{sc}}^2}{R^4} + \dots$$

for finite a_{sc} and positive constants α and β . Thus, the potentials can be fitted at some reasonably asymptotic distance (400–500 a.u. for these examples) and extrapolated to distances on the trap scale.

B. Hartree-Fock approximation

With the Hartree-Fock approximation, one seeks the best independent-particle wave function given the occupancy of each single-particle orbital. In the present case, we concentrate on the ground state of a system of bosons (i.e., the state in which all particles occupy the lowest orbital) although more general states can be considered. Considerable freedom exists in the choice of a single-particle basis set. This flexibility is used to derive an equation that determines those single-particle states which variationally minimize the total energy. In other words, the Hamiltonian is approximately diagonalized, including as much of the interparticle interac-

tions as is possible given that the trial wave function is constrained to independent-particle form.

The Hartree-Fock equation can be derived from either first- or second-quantized formalisms. Each provides separate and useful insights. The first-quantized derivation provides a simple picture that can be easily understood in terms of basic quantum mechanics. The second-quantized derivation, on the other hand, provides greater insight into the physics included in the trial wave function. Both approaches, of course, yield identical results.

We present the first-quantized derivation here and refer the interested reader to Ref. [19] for a second-quantized derivation. In many respects, the derivation presented here parallels the derivation of the Hartree-Fock equations for fermions (see Cowan [20], for example). The ansatz for the total ground-state wave function Φ in the independent-particle approximation is

$$\Phi(\mathbf{r}_1, \dots, \mathbf{r}_N) \approx \psi_0(\mathbf{r}_1) \cdots \psi_0(\mathbf{r}_N), \quad (6)$$

where the single-particle orbitals ψ_0 are to be determined. The spin part of the wave function is similarly a product of the spin kets for each atom and otherwise does not enter the calculation. The equation for ψ_0 results from an application of the variational principle to the Hamiltonian

$$H = \sum_{i=1}^N H_0(\mathbf{r}_i) + \sum_{i < j}^N V(\mathbf{r}_i - \mathbf{r}_j). \quad (7)$$

In this expression, the one-particle operator $H_0(\mathbf{r})$ includes the trapping potential and is given by

$$H_0(\mathbf{r}) = -\frac{\hbar^2}{2m} \nabla^2 + \frac{1}{2} m \omega^2 r^2.$$

The analogy to atomic structure calculations can be seen at this point if the trapping potential is replaced by the electron-nucleus Coulomb interaction. The two-particle operator $V(\mathbf{x}_i - \mathbf{x}_j)$ in Eq. (7) is the particle-particle interaction. In the case of neutral trapped atoms, it is a typical diatom interaction potential, while in atomic structure calculations, it is just the electronic Coulomb repulsion.

For the trial wave function in Eq. (6), the expectation value of the Hamiltonian [Eq. (7)] is

$$E_0^{\text{HF}} = N \frac{\langle \psi_0 | H_0 | \psi_0 \rangle}{\langle \psi_0 | \psi_0 \rangle} + \frac{N(N-1)}{2} \frac{\langle \psi_0 \psi_0 | V | \psi_0 \psi_0 \rangle}{\langle \psi_0 | \psi_0 \rangle^2}.$$

The one-particle matrix element is

$$\langle \psi_0 | H_0 | \psi_0 \rangle = \int d^3 r \psi_0^*(\mathbf{r}) H_0(\mathbf{r}) \psi_0(\mathbf{r}),$$

and the two-particle matrix element involves a double integral over the coordinates of two particles

$$\begin{aligned} \langle \psi_0 \psi_0 | V | \psi_0 \psi_0 \rangle &= \int d^3 r \int d^3 r' \psi_0^*(\mathbf{r}) \psi_0^*(\mathbf{r}') \\ &\quad \times V(\mathbf{r} - \mathbf{r}') \psi_0(\mathbf{r}) \psi_0(\mathbf{r}'). \end{aligned}$$

Taking the variation of E with respect to ψ_0^* gives, after some algebra,

$$\begin{aligned} \frac{\delta E_0^{\text{HF}}}{N} &= \frac{\langle \delta \psi_0 | H_0 | \psi_0 \rangle}{\langle \psi_0 | \psi_0 \rangle} + \frac{(N-1)}{2} \frac{\langle \delta \psi_0 \psi_0 + \psi_0 \delta \psi_0 | V | \psi_0 \psi_0 \rangle}{\langle \psi_0 | \psi_0 \rangle^2} \\ &\quad - \left(\frac{E_0^{\text{HF}}}{N} - \frac{(N-1)}{2} \frac{\langle \psi_0 \psi_0 | V | \psi_0 \psi_0 \rangle}{\langle \psi_0 | \psi_0 \rangle^2} \right) \frac{\langle \delta \psi_0 | \psi_0 \rangle}{\langle \psi_0 | \psi_0 \rangle}. \end{aligned}$$

For arbitrary variations $\delta \psi_0^*$, the stationary condition $\delta E_0^{\text{HF}} = 0$ subject to $\langle \psi_0 | \psi_0 \rangle = 1$ is satisfied when

$$[H_0(\mathbf{r}) + V_{\text{HF}}(\mathbf{r})] \psi_0(\mathbf{r}) = \varepsilon_0 \psi_0(\mathbf{r}), \quad (8)$$

where the mean field V_{HF} is given by

$$V_{\text{HF}}(\mathbf{r}) = (N-1) \int d^3 r' \psi_0^*(\mathbf{r}') V(\mathbf{r} - \mathbf{r}') \psi_0(\mathbf{r}'). \quad (9)$$

For a small number of atoms, the factor $N-1$ is critical for comparisons with number-conserving solutions. Using the standard factor of N_0 present in the Gross-Pitaevskii treatment [21–23] will lead to order N^{-1} differences as found in Ref. [24]. The eigenenergy ε_0 in Eq. (8) is defined as

$$\varepsilon_0 = \frac{E_0^{\text{HF}}}{N} + \frac{(N-1)}{2} \langle \psi_0 \psi_0 | V | \psi_0 \psi_0 \rangle \quad (10)$$

and is just the ground-state orbital energy.

Interestingly, ε_0 obeys Koopmans theorem [25] as do the orbital energies for fermions. The statement of Koopmans theorem applicable to a system of bosons is that the orbital energy represents the difference between the Hartree-Fock ground-state energy for N particles and $N-1$ particles provided the difference between the ground-state orbital for N particles and the ground-state orbital for $N-1$ orbitals can be neglected. In the limit $N \gg 1$, the latter approximation is physically reasonable given the order N^{-1} effect of a single additional particle on the orbital. In fact, Koopmans theorem holds quite well for as few as 10 particles. From the above statement, it can also be recognized that Koopmans theorem is essentially a statement of the definition of the chemical potential encountered in the Gross-Pitaevskii equation. From Eq. (10), the total energy for a system of N particles can be written as

$$E_0^{\text{HF}} = N \langle \psi_0 | H_0 | \psi_0 \rangle + \frac{N(N-1)}{2} \langle \psi_0 \psi_0 | V | \psi_0 \psi_0 \rangle.$$

The energy difference between a system with N particles and one with $N-1$ is thus

$$\begin{aligned} E_0^{\text{HF}}(N) - E_0^{\text{HF}}(N-1) \\ = \langle \psi_0 | H_0 | \psi_0 \rangle + (N-1) \langle \psi_0 \psi_0 | V | \psi_0 \psi_0 \rangle = \varepsilon_0. \end{aligned}$$

Thus, Koopmans theorem is also satisfied by bosons.

C. Configuration interaction

A further connection to standard atomic structure methods can be made through an application of configuration interac-

tion methods [20] to the system of bosons (see Ref. [24]). The term ‘‘configuration’’ in this context means a given set of occupation numbers $\{n_i\}$ corresponding to a set of single-particle orbitals $\{\psi_i(\mathbf{x})\}$. Configuration interaction, then, is the variational approach in which the trial wave function is expanded on a complete basis of many-body wave functions—or configurations—including the ground state and singly to multiply excited configurations. Since this is a complete many-body basis, the exact, time-independent, many-body energy eigenstates can in principle be calculated. In practice, of course, the expansion must be limited to a finite number of basis functions.

For three bosons, the configuration interaction wave function consists of the ground state, singly excited states, doubly excited states, and triply excited states. This can be written explicitly as

$$|\Psi\rangle = a_0|n_0=3\rangle + \sum_{p \neq 0} a_p|n_0=2,1_p\rangle \\ + \sum_{p,p' \neq 0} b_{pp'}|n_0=1,1_p,1_{p'}\rangle \\ + \sum_{p,p',p'' \neq 0} c_{pp'p''}|n_0=0,1_p,1_{p'},1_{p''}\rangle,$$

where the notation 1_p indicates that the p th single-particle orbital is occupied by one boson, i.e., $n_p=1$. This wave function is thus the most general completely symmetric three-body wave function. Upon truncation, the variational principle for the total energy yields the matrix eigenvalue problem

$$\mathbf{H}\Psi_\nu = E_\nu\Psi_\nu,$$

where Ψ_ν is the vector of expansion coefficients. To efficiently diagonalize the Hamiltonian matrix \mathbf{H} , only those configurations that contribute most should be included, since the number of configurations can be quite large even for three atoms. Haugset and Haugerud, for instance, obtained matrices up to order 80 000 for a few tens of particles in one and two dimensions.

The first step in choosing the most efficient configuration basis is to adopt the best single-particle basis. One near optimal single-particle basis is obtained by solving

$$\left(-\frac{\hbar^2}{2m} \frac{d^2}{dr^2} + \frac{l(l+1)}{2mr^2} + \frac{1}{2}m\omega^2 r^2 + V_{\text{HF}} \right) R_{nl} = \varepsilon_{nl} R_{nl}, \quad (11)$$

where the angular part of the orbital is just a spherical harmonic, $Y_{lm}(\theta, \phi)$. The mean-field term lifts the degeneracy in l , but the degeneracy in m remains. For $(n, l, m) = (0, 0, 0)$, Eq. (11) is just the Hartree-Fock equation for the ground-state orbital, while for all other (n, l, m) it is a linear equation with an effective potential that includes the mean field. To reduce the number of configurations, we use three criteria based upon the orbital properties determined by Eq. (11).

Our first criterion for inclusion of a given configuration is based upon its symmetry. We expect that the exact ground

state has zero total orbital angular momentum L and thus zero total angular momentum projection M_L . While the configurations are not themselves eigenstates of total angular momentum, only those that have components of $L=0$ and $M_L=0$ are included. Similarly, only even total parity configurations are included in the expansion. The maximum single-particle angular momentum and energy can also be varied independently of these requirements and each other—a facility that we take advantage of in the present studies.

Our second criterion is based upon the structure of the Hamiltonian matrix. To simplify the visualization of the Hamiltonian matrix, we can partition it into submatrices according to the states that the submatrix couples. The ground state will be labeled with a G , singly excited states with an S , doubly excited states with a D , and triply excited states with a T . Explicitly,

$$\mathbf{H} = \begin{pmatrix} H_{GG} & H_{GS} & H_{GD} & H_{GT} \\ H_{SG} & H_{SS} & H_{SD} & H_{ST} \\ H_{DG} & H_{DS} & H_{DD} & H_{DT} \\ H_{TG} & H_{TS} & H_{TD} & H_{TT} \end{pmatrix}.$$

Since only two-body interactions are included, the submatrices H_{GT} and H_{TG} are zero. Also, since we use the single-particle basis defined by the ground-state Hartree-Fock equation, the submatrices H_{GS} and H_{SG} vanish by Brillouin’s theorem. The Hamiltonian is thus

$$\mathbf{H} = \begin{pmatrix} H_{GG} & 0 & H_{GD} & 0 \\ 0 & H_{SS} & H_{SD} & H_{ST} \\ H_{DG} & H_{DS} & H_{DD} & H_{DT} \\ 0 & H_{TS} & H_{TD} & H_{TT} \end{pmatrix}. \quad (12)$$

The selection of configurations is greatly simplified by the fact that we are only interested in the ground-state energy. Examination of Eq. (12) shows that the contribution of triple excitations to the ground-state energy enters first at fourth order (in a Rayleigh-Ritz perturbation scheme, for instance). Because we will consider systems in which the deviation from noninteracting is minor, triple excitations can be neglected—a huge reduction in the number of configurations. A typical case is shown in Table I. Eliminating triple excitations in this calculation reduced the matrix size by more than a factor of 7. Numerical checks confirm that triple excitations affect the ground-state energy only beyond the level of accuracy that interests us here. For the parameters of Table I, for instance, the total ground-state energy calculated with triple excitations is $4.5364563 \hbar\omega$ and with only up to double excitations included $4.5364564 \hbar\omega$. Single excitations could have similarly been excluded from the calculation since they also enter first at fourth order for the ground-state energy, but the resulting reduction in the number of configurations would normally be less than 1% (see Table I). Note that while the decoupling of single excitations from the ground state depends on the single-particle basis, the decoupling of triple excitations depends only on the fact that two-body excitations are included. For other single-particle bases,

TABLE I. The number of singly, doubly, and triply excited configurations for three ^{87}Rb atoms in a 1 kHz isotropic trap. The scattering length is taken to be 100 a.u. The total orbital angular momentum is zero and the total parity is even. Only s waves are allowed for the orbital wave functions, and excitation energies up to $300\hbar\omega$ are included. The orbitals were calculated within a spherical box of radius $5\sqrt{\hbar/m\omega}$.

Number of excitations	Number of configurations
0	1
1	37
2	544
3	4511
Total	5093

however, triple excitations typically contribute a larger fraction to the ground-state energy even though they still enter first at fourth order.

Our third criterion involves the energies of the orbitals making up a given configuration. The expansion includes all states consistent with the above criteria up to a given configuration energy. The configuration energy is just the expectation value of the Hamiltonian for a particular configuration, in other words the diagonal element of Eq. (12). As in Eq. (10), the configuration energy is not simply the sum of the energies of the orbitals comprising the configuration, but includes corrections for double counting of two-body interaction energies. Nevertheless, the orbital energies prove to be a useful guide for including a configuration. We show in Fig. 1 the contribution of each configuration to the total energy of the ground state of the three-particle system as a function of the difference in orbital energies. The ground orbital energy is excluded from the difference, and a configuration's contribution is measured by the product of the configuration en-

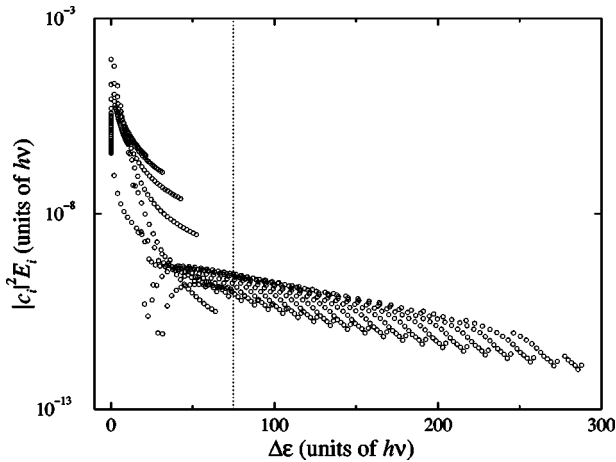


FIG. 1. The diagonal contribution of each configuration to the total energy for three ^{87}Rb atoms in a 1 kHz isotropic trap. The product of the configuration energy E_i and the square of the configuration interaction expansion coefficient c_i as a function of $\Delta\varepsilon$. The dotted line at $\Delta\varepsilon = 75h\nu$ indicates the cutoff used in the calculations. The basis parameters are as in Table I except that only up to double excitations were included.

ergy and the square of the expansion coefficient obtained from a full calculation. So, recalling that only up to double excitations are allowed, this difference is just the difference in the orbital energies of the two excited particles. For example, if a configuration consists of orbitals (0,0,0), (4,0,0), and (10,0,0), then the relevant energy difference is $\Delta\varepsilon = |\varepsilon_{4,0} - \varepsilon_{10,0}|$. The parameters used for Fig. 1 are the same as for Table I except that triple excitations are excluded. It is evident from the figure that most configurations with large $\Delta\varepsilon$ contribute very little to the total energy. It is also evident that if we are only interested in obtaining four to five digits of the total ground-state energy, then we can exclude from the calculation all of those configurations having a $\Delta\varepsilon$ greater than about $75\hbar\omega$. When the maximum allowed configuration energy is large as in the figure, this translates into a large reduction in the number of configurations—almost a factor of 2 for the parameters of the figure, or from 582 to 313. The total energy calculated after the reduction is $4.5364564\hbar\omega$, which is identical to the energy before the reduction.

In order to test the convergence of the expansion with respect to the maximum configuration energy, it is necessary to be able to include very-high-energy configurations (energies up to several hundred $\hbar\omega$). Given that the spectrum of Eq. (11) is roughly similar to that of a harmonic oscillator, the number of states necessary to form a complete set up to some energy is proportional to that energy. This number quickly becomes unmanageable, and a further reduction must be sought. Our solution, since we are interested only in the ground state at this point, is to solve for the single-particle states within a box that is just large enough to contain the ground-state orbital. The energy spectrum with this boundary condition quickly switches from the oscillatorlike linear dependence of the orbital energy on the principle quantum number n to a boxlike quadratic dependence. The number of states necessary to obtain a complete set of single-particle states up to a given energy over this restricted space thus scales like the square root of that energy. Numerical tests for the modest maximal configuration energies attainable without the box show that the ground-state energy is unaffected by the box boundary condition.

III. RESULTS AND DISCUSSION

Use of the pseudopotential based on the known s -wave atom-atom scattering length reproduces the two-body scattering wave function at large atomic separations. This is a physically intuitive approach, but it can also be viewed from the rather different and more mathematical perspective of many-body perturbation theory. In this language, a many-body problem is written in terms of some independent-particle basis and the interactions accounted for in a perturbation expansion. Each term of the expansion can then be represented diagrammatically. The general goal of this approach is to include as many of these diagrams as possible in a given calculation. Several techniques have been devised, in fact, to include particular classes of diagrams to infinite order in the interaction. The Hartree-Fock and random-phase approximations are two such techniques which sum different classes of diagrams to all orders. For two-body interactions with a very strongly repulsive core, however, an additional

class of diagrams must be taken into account. These diagrams represent repeated two-body interactions and correspond to the usual Born series in scattering theory. In the first Born approximation, the s -wave scattering length is

$$a_B = \frac{\mu}{2\pi\hbar^2} \int d^3r V(\mathbf{r}),$$

where μ is the reduced mass and $V(\mathbf{r})$ is the two-body interaction. Summing the Born series within the many-body perturbation theory expansion essentially amounts to replacing the first Born scattering length above by the scattering length obtained in a two-body scattering calculation. Note that such a replacement is valid only in the low-density limit. It is this process that has led others in this field to simply write the two-body interaction in the Hamiltonian in the form of a Fermi contact potential. (For a full development specifically for trapped gases, see Proukakis *et al.* [1].) A more general effective interaction theory has been developed by Brueckner and others to handle strongly repulsive two-body interactions including the effects of the mean field [26–28].

One way to see the importance of these considerations is to examine the mean-field term from the Hartree-Fock equation, Eq. (8). The orbital $\psi_0(\mathbf{r})$ varies slowly on the scale of $V(\mathbf{r})$ (s -wave scattering), whereby $V_{\text{HF}}(\mathbf{r})$ can be approximately rewritten as

$$\begin{aligned} V_{\text{HF}}(\mathbf{r}) &\approx (N-1) |\psi_0(\mathbf{r})|^2 \int d^3r' V(\mathbf{r}-\mathbf{r}') \\ &= (N-1) \frac{2\pi\hbar^2 a_B}{\mu} |\psi_0(\mathbf{r})|^2. \end{aligned}$$

Because of the large repulsive core in $V(r)$, a_B is a large positive number regardless of the other details of the potential. It is this result that leads to the rather counterintuitive conclusion that using a realistic two-body potential in the Hartree-Fock equation yields a much poorer approximation than using a δ -function potential. Thus, it is not only *convenient* to make the shape-independent approximation but actually *essential* in order to obtain quantitatively correct results.

Interestingly, the solution of the Hartree-Fock equation, using a Morse interaction potential, is not accurate even in the high-density limit where it might be expected that the structure of the two-body interaction plays a more important role. The difficulty of the hard core remains, however, and the simple product form of the wave function is not sufficiently flexible to account for the correlated exclusion of the wave function from the hard-core region. This is the analog of the well known cusp problem from atomic and molecular structure. The difference here is that instead of reaching a finite value with a discontinuous first derivative at the two-body coalescence points, the wave function is merely suppressed in the classically forbidden region under the hard core of the two-body interaction. So, for instance, many-body bound states cannot be obtained using realistic two-body interactions in the Hartree-Fock equation.

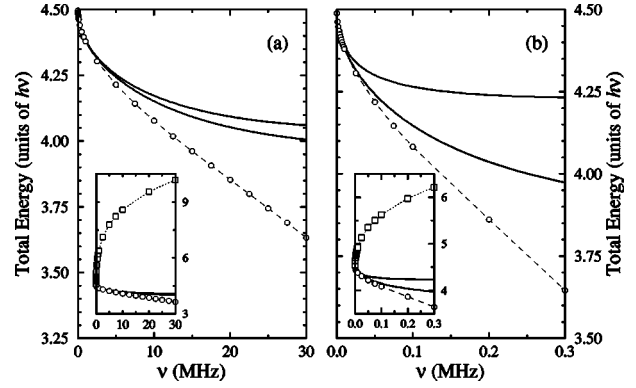


FIG. 2. Comparison of the total ground-state energy calculated using the Hartree-Fock and adiabatic hyperspherical approximations for the negative scattering lengths (a) $a_{\text{sc}} = -10$ a.u. and (b) $a_{\text{sc}} = -100$ a.u. as a function of trapping frequency. The dashed line with circles corresponds to the pseudopotential Hartree-Fock result and the two solid lines to the lower and upper bounds provided by the hyperspherical analysis. The insets expand the energy scale to include the result of the Hartree-Fock approximation with Morse two-body interactions (dotted line with squares).

A. Ground-state energies

Since the pseudopotential approximation is valid only in the low-density limit, i.e., $na_{\text{sc}}^3 \ll 1$ or $n4\pi\hbar^2 a_{\text{sc}}/m \ll \hbar\omega$, we should expect to see deviations from the exact result as the density is increased. Accordingly, we document these deviations in Figs. 2 and 3. The total ground-state energy as a function of trap frequency is shown for four cases: $a_{\text{sc}} \approx -100$ a.u., -10 a.u., 10 a.u., and 100 a.u. In each case, the lower and upper bounds determined from the hyperspherical approach are indicated by thick solid lines and the Hartree-Fock with pseudopotential result is indicated by a dashed line. The scattering lengths used in the Hartree-Fock calculation corresponded to the exact scattering length a_{sc} calculated for the Morse potentials used in the hyperspherical calculation. The precise values of the scattering lengths are

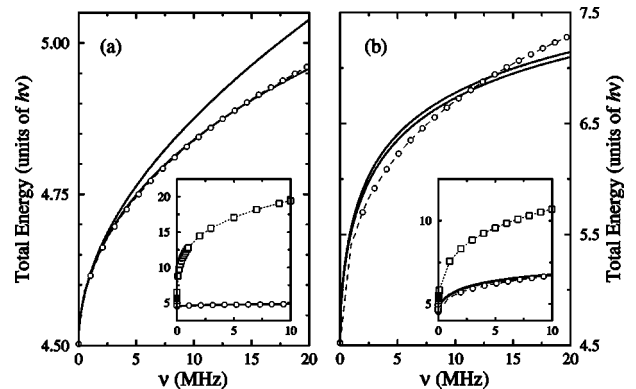


FIG. 3. Comparison of the total ground-state energy calculated using the Hartree-Fock and adiabatic hyperspherical approximations for the positive scattering lengths (a) $a_{\text{sc}} = 10$ a.u. and (b) $a_{\text{sc}} = 100$ a.u. as a function of trapping frequency. The dashed line with circles corresponds to the Hartree-Fock result and the two solid lines to the lower and upper bounds provided by the hyperspherical analysis. The insets expand the energy scale to include the result of the Hartree-Fock approximation with Morse two-body interactions (dotted line with squares).

−98.220 a.u., −9.9226 a.u., 10.023 a.u., and 99.798 a.u. (corresponding to $D=1.74\times 10^{-7}$ a.u., 1.09×10^{-7} a.u., 1.18×10^{-6} a.u., and 2.197×10^{-7} a.u., respectively). As expected, the two approaches yield similar results in the low-density (low trap frequency) regime, but the Hartree-Fock energy is consistently close to the hyperspherical bounds only for $a_{sc}\approx 10$ a.u., Fig. 3(a). Interestingly, both positive scattering length cases are closer to the exact bounds than the negative scattering length cases. The physical origin of this difference can be understood by recalling the relation between the phase shift and scattering length—a negative scattering length means that the two-body scattering wave function is shifted towards smaller r relative to the noninteracting wave function, while a positive scattering length means that the wave function is shifted towards larger r . The negative scattering length wave function thus samples the two-body potential more than the positive scattering length wave function.

It is worth pointing out that the results shown in Figs. 2 and 3 will almost certainly change quantitatively for different choices of model potentials. We do not expect that they will change qualitatively, though, provided the model potential is short-ranged.

To illustrate the importance of including the correct two-body scattering physics, we solve the Hartree-Fock equation, Eq. (8), “directly” using realistic two-body Morse interactions as in the adiabatic hyperspherical approximation (see Sec. II A). This is simplified by the fact that for s -wave orbitals the angular integrals in the Hartree-Fock potential can be analytically evaluated. The integrals and the resulting Hartree-Fock equation are given in Appendix A. The Hartree-Fock equation is thus reduced to a one-dimensional equation with a nonlocal potential Eq. (A1). Solving this equation with $D=1.74\times 10^{-7}$ a.u. gives for three atoms in a 1 kHz trap a total energy of $4.645\hbar\omega$. This choice of D clearly exposes the shortcoming of using a realistic two-body potential because it corresponds to a scattering length a_{sc} that is *negative*—a relatively large negative scattering length of −98.22 a.u., in fact. For a negative scattering length, the total energy is expected to be lower than the noninteracting value of $4.5\hbar\omega$, rather than larger. At $4.464\hbar\omega$, the upper bound on the exact energy calculated using the hyperspherical approach is consistent with this expectation. The higher energy obtained with the Morse potential is, however, consistent with the fact that the Born scattering length for these parameters is large and positive, 407.5 a.u. The dotted lines with square symbols in the insets of Figs. 2 and 3 show more extensive results of the Hartree-Fock approximation with Morse two-body interactions. As discussed above, the total energies are spectacularly bad over the whole range of trap frequencies. For the negative scattering length cases shown in Fig. 2, even the qualitative behavior is incorrect. For $a_{sc} = -10$ a.u., just as for $a_{sc} = -100$ a.u., this failure can be traced back to the fact that the Born scattering length is large and positive (255.3 a.u.).

The interpretation of Fig. 2(b) is complicated by the presence of a bound three-body state for this choice of potential parameters, even in the absence of the trap. This state lies in the inner well of the potential shown as a dotted line in Fig. 4 which has a depth of between 9 and 14 mK (upper and lower bounds, respectively). In fact, because there are no

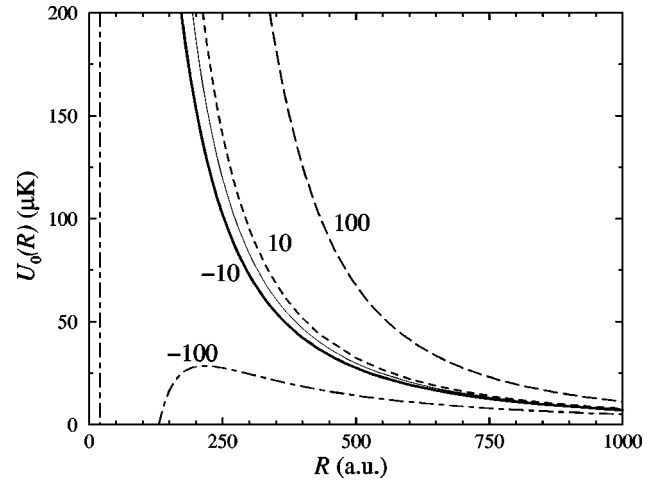


FIG. 4. The adiabatic hyperspherical potential curves that correlate to three free atoms for different two-body scattering lengths (in a.u.) as indicated in the figure. The thin solid line midway between the $a_{sc}=10$ a.u. and $a_{sc}=-10$ a.u. curves indicates the noninteracting hyperspherical potential. Note that the lowest curve in the figure, for $a_{sc}=-100$ a.u., has a well approximately 10 mK deep at small R that is not shown.

two-body bound states, this is an example of a halo state. Loosely bound three-body states that exist when no two of the particles are separately bound are called halo states and are a well-studied phenomenon in nuclear physics. Examination of the wave function for the three-body bound state shows that it has a very large spatial extent with a mean hyperradius on the order of a few hundred atomic units. Even so, this state is well localized on the scale of the trap since the classical turning point for the noninteracting oscillator at the highest frequency considered in Fig. 2(b) is still nearly 4000 a.u. Physically, this state represents a bound trimer whose center of mass obeys a simple harmonic-oscillator equation. We would thus associate the first excited state with the “condensate ground state” in a trap since the majority of its probability density lies beyond the potential barrier.

It has recently been emphasized that the pseudopotential approach is not valid if many-body bound states exist in the problem when the trap is turned off. Given our labeling of the first excited state as the one relevant for the condensate “ground state” in a trap, we see from Fig. 2(b) that the Hartree-Fock with pseudopotential actually does quite well in the limit of low frequencies even in this case. Thus, the influence of a many-body bound state does not seem to be a serious problem for the pseudopotential approximation. This is reassuring since the true ground state for trapped alkali-metal gases is a many-body bound state just like the true ground state in this three-body example. Figure 5 shows the behavior of the total energy of the bound state as a function of the trap frequency. When the $\frac{3}{2}\hbar\omega$ associated with the center-of-mass zero-point energy is taken into account, it is clear that the state remains a bound three-body state for even the highest trap frequency. Note that the lower limit on the bound-state energy remains negative over the entire frequency range plotted and is not shown. The height of the barrier (see the dotted line in Fig. 4) is also indicated in the figure as a long dashed line. For frequencies above about 220 kHz, the first excited state [the state shown in Fig. 2(b)] is

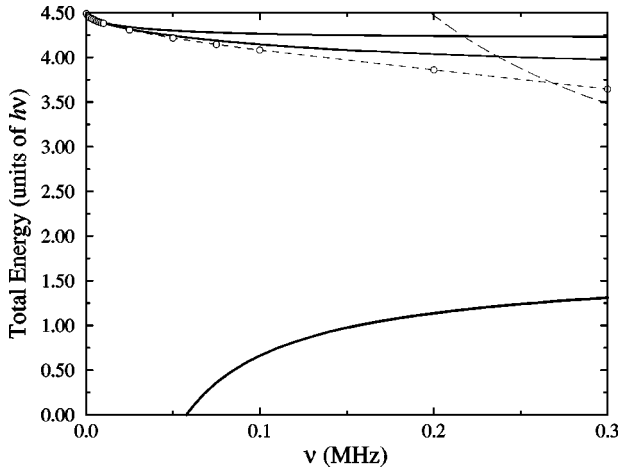


FIG. 5. Expanded view of Fig. 2(b) showing also the total energy of the three-body state bound in the inner well of the potential in Fig. 4. The dashed line with circles corresponds to the Hartree-Fock result and the upper two solid lines to the lower and upper bounds provided by the hyperspherical analysis. The thick solid line indicates the energy of the three-body bound state, and the thin dashed line indicates the height of the potential barrier (see Fig. 4).

above the potential barrier. At this point, the identification of this state as the one relevant for trapping fails, and, in a system in which two-body bound states exist, this passage over the barrier would correspond to the collapse of the condensate as spin-flipping processes and three-body recombination would destroy the condensate. It is interesting to note that the Hartree-Fock energy is showing no sign of the instability. In fact, the critical frequency predicted from the Hartree-Fock formula

$$(N-1) \frac{|a_{sc}|}{\beta} = 0.57497$$

with $\beta = \sqrt{\hbar/m\omega}$ is 2 MHz—about an order of magnitude too large.

For the positive scattering length cases, it was similarly necessary to identify an excited state as the relevant state instead of the ground state. The reason in these cases was the presence of two-body bound states. Here, however, it is the potential curves in Fig. 4 which are not the ground state. There are lower-lying curves which correlate asymptotically with a molecule plus free atom. We are interested in states which correlate to three free atoms. Further, the lower-lying potential curves support three-body bound states. But, as in the case of the negative scattering length above, the presence of many-body bound states does not seem to degrade the pseudopotential approximation for low frequencies.

The differences between the Hartree-Fock and hyperspherical results at higher densities can be attributed primarily to two effects neglected in the pseudopotential approximation. The first is the lack of energy dependence in the scattering length. As the trap is made tighter, the mean collision energy is increased, making the s -wave scattering length approximation poorer. The second effect neglected in the pseudopotential approximation is the influence of the many-body system on the two-body collision. One example of this influence can be seen in the three-body system. If the

third atom is nearby during a two-body collision, then the collision energy is affected by the interaction with that third atom. When more particles are present, of course, more complicated processes can occur.

B. Breakdown of the pseudopotential as an exact Hamiltonian

The Hamiltonian used in calculations for atomic BEC experiments has routinely been written as

$$H = \sum_i^N H_0(\mathbf{x}_i) + \frac{4\pi\hbar^2 a_{sc}}{m} \sum_{i<j}^N \delta(\mathbf{x}_i - \mathbf{x}_j), \quad (13)$$

leading some to use this as an exact Hamiltonian for the many-body system. It has been emphasized previously [1] that this Hamiltonian should not be used for exact calculations, and we stress it again here. If the above Hamiltonian is applied to a two-particle system, the problem becomes clear. Appendix B shows one way to see the pathological nature of this form of the interaction potential when used as a model of the full Hamiltonian of the system. Even perturbative formulations are not exempt from the pathology, as evidenced by the fact that one can prove that the energy correction in second-order perturbation theory diverges for a three-dimensional Dirac δ -function interaction potential. In a different context [29], it has also been shown that divergent series arise when this type of an interaction potential is treated using a partial wave expansion of the multichannel scattering solution.

The problems with this δ -function potential can also be seen from Fig. 6, where we present the outcome of an extensive numerical study of the convergence of a configuration interaction calculation based on Eq. (13) as the “exact” Hamiltonian. The details of our calculation were described above in Sec. II C. The results shown are for three ^{87}Rb atoms in a 1 kHz trap with a scattering length of 100 a.u. Using all of the basis-set reduction techniques described in Sec. II C, we calculated the total ground-state energy as a function of the maximum orbital energy and maximum angular momentum per orbital allowed in the configurations. The maximum angular momentum per orbital is fixed at the indicated value for the eight curves in Fig. 6(a). For instance, the $l_{\max} = 3$ curve includes orbitals with $l = 0, 1, 2,$ and 3 . Each of these eight curves converges in the limit of infinite orbital energy, but to a different value. The fully converged energy of the ground state would then be the limit of these extrapolated values as $l_{\max} \rightarrow \infty$. In Fig. 6(b), we show the extrapolated values of each curve in Fig. 6(a) as a function of l_{\max} . The extrapolation was accomplished by a least-squares fitting of the form

$$E_0(\varepsilon_{\max}, l_{\max}) = E_0(\infty, l_{\max}) + \frac{\alpha}{\varepsilon_{\max}^\beta}.$$

Only those portions of the curves at $\varepsilon_{\max} \geq 210\hbar\omega$ were included in the fitting. The curve in Fig. 6(b) is not showing any evidence of converging in the limit $l_{\max} \rightarrow \infty$.

It is clear, then, that the δ function is not suitable as an exact potential in a three-dimensional system. When approximations are made, however, finite results can be obtained. In the present case, each curve in Fig. 6(a) converges

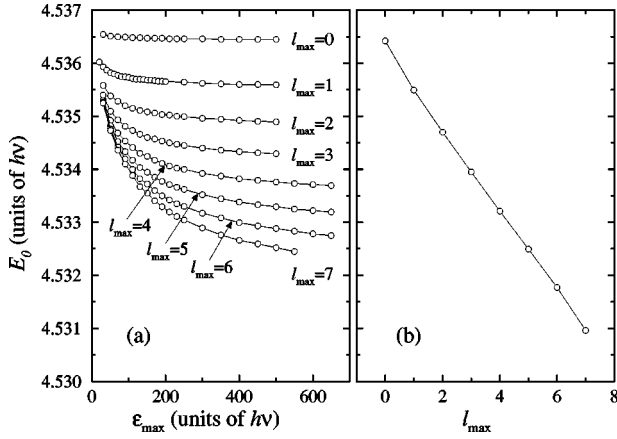


FIG. 6. Convergence of the configuration interaction expansion for three ^{87}Rb atoms in a 1 kHz isotropic trap. Each curve in (a) shows the convergence of the total ground-state energy as a function of the maximum orbital energy for various values of l_{max} . The extrapolation of these curves to $\varepsilon_{\text{max}} \rightarrow \infty$ yields the points in (b). The error in the extrapolation is roughly the size of the symbols in (b).

nically to some value when l_{max} is fixed. Similarly, if the ground-state energy is plotted as a function of l_{max} with ε_{max} fixed, the curves each converge.

Some authors, including Huang and Tommasini [30] and Demkov and Ostrovskii [31], have bypassed the δ -function pathologies by changing the interaction $V\psi$ into the following form:

$$V(\mathbf{r}_i - \mathbf{r}_j)\psi = \frac{2\pi\hbar^2 a_{\text{sc}}}{\mu} \delta(|\mathbf{r}_i - \mathbf{r}_j|) \frac{\partial(|\mathbf{r}_i - \mathbf{r}_j|\psi)}{\partial(|\mathbf{r}_i - \mathbf{r}_j|)},$$

where μ is the two-body reduced mass and a_{sc} is the scattering length. This form of the interaction leads to a non-Hermitian Hamiltonian unless the class of wave functions allowed in Hilbert space is constrained to obey the following boundary condition near every coalescence point in configuration space:

$$\psi(\mathbf{r}_i - \mathbf{r}_j)_{\mathbf{r}_i \rightarrow \mathbf{r}_j} \rightarrow C_{ij} \left(\frac{1}{|\mathbf{r}_i - \mathbf{r}_j|} - \frac{1}{a_{\text{sc}}} \right),$$

with C_{ij} an arbitrary normalization constant. In practice, this boundary condition cannot be readily imposed when utilizing the independent-particle many-body trial wave functions that are convenient for the description of the ground state and excited states of a Bose-Einstein condensate. The boundary condition constraint could be applied to solutions written in the Jastrow form, however, which includes $\mathbf{r}_{ij} = \mathbf{r}_i - \mathbf{r}_j$ as an explicit coordinate in the wave function. But this form appears to be useful only for calculations of the condensate ground state. In any event, we do not view the methods of Refs. [30,31] as providing a solution which can bypass the δ -function pathologies documented above and in Appendix B, except possibly for Jastrow-type descriptions of the ground state.

Even if we could ignore the δ -function interaction pathologies, the configuration interaction approach has a second problem. The point of CI is to account for interactions not already diagonalized by the basis set. Since the residual

interactions are essentially the two-body terms, CI can be thought of as accounting (eventually) for two-body collisions. But, by writing the coefficient of the δ function as the scattering length a_{sc} , the two-body collisions have been accounted for to infinite order *via* the Born series. When used with Eq. (13), the CI approach thus “double counts” the effects of two-body interactions.

IV. SUMMARY

While it is not straightforward to extrapolate the above results for three atoms to the general case of N atoms, the results document a breakdown in the pseudopotential approximation that should occur when the density grows large. We have shown that such a breakdown definitely occurs in the three-body case. And, if the dependence of the Hartree-Fock solutions on the combination $Na_{\text{sc}}\sqrt{\omega}$ is considered, then the breakdown frequencies presented here might translate into a semiquantitative estimate of the critical number for condensates with more atoms. We have also shown the result of using the pseudopotential as if it constitutes an “exact Hamiltonian.” In particular, the three-dimensional δ function causes the ground-state energy to diverge as the number of basis functions is increased. For the one-dimensional case studied by Haugset *et al.*, these divergences are absent, and a well behaved exact solution is possible. Already in their two-dimensional study, however, divergences can be expected as the expansions approach completeness.

ACKNOWLEDGMENTS

B.D.E. thanks the National Science Foundation for support through the Institute for Theoretical Atomic and Molecular Physics. The work of C.H.G. was supported in part by the U.S. Department of Energy, Office of Basic Energy Sciences.

APPENDIX A: HARTREE-FOCK WITH MORSE INTERACTIONS

At first thought, a direct solution of the Hartree-Fock equation, Eq. (8), with no approximation for $V(\mathbf{r})$ in Eq. (9) would seem to be an improvement over the seemingly severe approximation $V(\mathbf{r}) \rightarrow \gamma\delta(\mathbf{r})$ with γ some strength parameter. The Morse potential Eq. (5) is ideal for testing this proposition since the mean-field interaction integral can be performed in part analytically. The $\psi_0(\mathbf{r})$ is assumed to have the form

$$\psi_{000}(\mathbf{r}) = R_{00}(r) Y_{00}(\theta, \phi) = \frac{R_{00}(r)}{\sqrt{4\pi}}.$$

The mean-field term in Eq. (9) is explicitly written as

$$V_{\text{HF}}(\mathbf{r}) = (N-1) \int dr' r'^2 |R_{00}(r')|^2 \int \frac{d\Omega'}{4\pi} \frac{V(|\mathbf{r} - \mathbf{r}'|)}{\hbar\omega}.$$

The angular integrals in $V_{\text{HF}}(\mathbf{r})$ can be evaluated analytically for the Morse potential Eq. (5). The result is

$$V_{\text{HF}}(r) = (N-1) \frac{D}{\alpha^2} \int_0^\infty r'^2 dr' \frac{|R_0(r')|^2}{r > r_<} \times \left[\frac{1}{8} \{F(2\alpha, r_0; r_> - r_<) - F(2\alpha, r_0; r_> + r_<)\} - \{F(\alpha, r_0; r_> - r_<) - F(\alpha, r_0; r_> + r_<)\} \right], \quad (\text{A1})$$

where

$$F(a, b; y) = e^{-a(y-b)}(1+ay).$$

In this expression, $r_>$ ($r_<$) indicate that the larger (smaller) of r and r' is to be used. Equation (8) can now be readily solved numerically. Its solution for a trap frequency on the order of 100 Hz, however, is identical (within the precision of our calculations) to the solution of the Hartree-Fock equation with the approximation $V(\mathbf{r}) \approx 4\pi\hbar^2 m^{-1} a_B \delta(\mathbf{r})$ because of the disparity in length scales. The first Born approximation to the scattering length for a Morse potential is given by

$$a_B = \frac{mD}{4\hbar^2 a_0 \alpha^3} e^{a r_0} (e^{a r_0} - 16). \quad (\text{A2})$$

With all quantities on the right-hand side in SI units, a_B will be in atomic units.

From Eq. (A2), it is clear that using a realistic potential directly in the Hartree-Fock equations will give quantitatively poor results since a_B is monotonic as a function of D . The physical scattering length, on the other hand, shows a tangential pole structure. The shortcoming is especially evident for negative scattering lengths since a_B will remain positive even in this case.

APPENDIX B: δ -FUNCTION PATHOLOGY

The pathology of a Dirac δ -function potential can be discerned from the following analysis. Consider the scattering of a single Schrödinger particle from the potential

$$V(\mathbf{r}) = V_0 \delta(\mathbf{r} - \mathbf{a}),$$

with \mathbf{a} some fixed point in space. If we denote the three-dimensional outgoing-wave free-particle Green's function by $G_0(\mathbf{r}, \mathbf{r}') \sim e^{ik|\mathbf{r}-\mathbf{r}'|}/|\mathbf{r}-\mathbf{r}'|$, then the integral form of the Schrödinger equation for a scattering state that represents an incident particle with wave vector \mathbf{k}_0 is

$$\psi(\mathbf{r}) = e^{i\mathbf{k}_0 \cdot \mathbf{r}} + \int d^3 r' G_0(\mathbf{r}, \mathbf{r}') V(\mathbf{r}') \psi(\mathbf{r}').$$

For the δ -function potential, this can be solved, giving

$$\psi(\mathbf{r}) = e^{i\mathbf{k}_0 \cdot \mathbf{r}} + V_0 G_0(\mathbf{r}, \mathbf{a}) \psi(\mathbf{a}),$$

in terms of an as-yet-undetermined constant $\psi(\mathbf{a})$. A consistency or continuity condition obtained by evaluating $\psi(\mathbf{r})$ in the limit $\mathbf{r} \rightarrow \mathbf{a}$ determines this ‘‘constant’’ to be the solution of

$$\psi(\mathbf{a}) = \frac{e^{i\mathbf{k}_0 \cdot \mathbf{a}}}{1 - V_0 G_0(\mathbf{a}, \mathbf{a})}.$$

The divergent nature of $G_0(\mathbf{a}, \mathbf{a})$ might appear to suggest that the only possible solution of the integral equation in three dimensions (more generally, in two or more dimensions) is obtained for $\psi(\mathbf{a}) = 0$. In fact, this does not solve the problem in a satisfactory manner, because that choice leads to $\psi(\mathbf{r}) = e^{i\mathbf{k}_0 \cdot \mathbf{r}}$, which does not obey the requirement $\psi(\mathbf{a}) = 0$, implying that this is not a consistent solution to the problem.

-
- [1] N.P. Proukakis, K. Burnett, and H.T.C. Stoof, *Phys. Rev. A* **57**, 1230 (1998).
- [2] K. Huang, *Statistical Mechanics* (Wiley, New York, 1963); K. Huang and C.N. Yang, *Phys. Rev.* **105**, 767 (1957).
- [3] A. Omont, *J. Phys. (Paris)* **38**, 1343 (1977).
- [4] E. Fermi, *Nuovo Cimento* **11**, 157 (1934).
- [5] C.D. Lin, *Phys. Rep.* **257**, 1 (1995).
- [6] Y. Zhou, C.D. Lin, and J. Shertzer, *J. Phys. B* **26**, 3937 (1993).
- [7] J. Avery, *Hyperspherical Harmonics: Applications in Quantum Theory* (Kluwer, Boston, 1989).
- [8] J. Macek, *J. Phys. B* **1**, 831 (1968).
- [9] B.M. Axilrod and E. Teller, *J. Chem. Phys.* **11**, 299 (1943).
- [10] M. Marinescu and A.F. Starace, *Phys. Rev. A* **55**, 2067 (1997).
- [11] C. de Boor, *A Practical Guide to Splines* (Springer, New York, 1978); C. de Boor, pppack, <http://netlib.bell-labs.com/netlib>.
- [12] R. Lehoucq, K. Maschhoff, D. Sorensen, and C. Yang, <http://www.caam.rice.edu/software/ARPACK>.
- [13] J.K. Cullum and R.A. Willoughby, *Lanczos Algorithms for Large Symmetric Eigenvalue Computations* (Birkhauser, Boston, 1985).
- [14] A. Starace and G.L. Webster, *Phys. Rev. A* **19**, 1629 (1979).
- [15] P.M. Morse and H. Feshbach, *Methods of Theoretical Physics: Part II* (McGraw-Hill, New York, 1953), p. 1671.
- [16] G. Herzberg, *Molecular Spectra and Molecular Structure: Vol. I* (van Nostrand, Toronto, 1950).
- [17] J.P. Burke, Jr. (private communication).
- [18] Z. Zhen and J. Macek, *Phys. Rev. A* **38**, 1193 (1988).
- [19] B.D. Esry, *Phys. Rev. A* **55**, 1147 (1997).
- [20] R.D. Cowan, *The Theory of Atomic Structure and Spectra* (University of California Press, Berkeley, 1981).
- [21] A.L. Fetter and J.D. Walecka, *Quantum Theory of Many-Particle Systems* (McGraw-Hill, New York, 1971).
- [22] V.L. Ginzburg and L.P. Pitaevskii, *Zh. Éksp. Teor. Fiz.* **34**, 1240 (1958) [*Sov. Phys. JETP* **7**, 858 (1958)]; E.P. Gross, *J. Math. Phys.* **4**, 195 (1963).
- [23] M. Edwards and K. Burnett, *Phys. Rev. A* **51**, 1382 (1995).
- [24] T. Haugset and H. Haugerud, *Phys. Rev. A* **57**, 3809 (1998).
- [25] T. Koopmans, *Physica (Amsterdam)* **1**, 104 (1933).
- [26] K.A. Brueckner and C.A. Levinson, *Phys. Rev.* **98**, 1445 (1955).
- [27] K.A. Brueckner and K. Sawada, *Phys. Rev.* **106**, 1117 (1957).

- [28] J. Goldstone, Proc. R. Soc. London, Ser. A **239**, 267 (1957).
- [29] N.Y. Du and C.H. Greene, Phys. Rev. A **36**, 971 (1987); see also **36**, 5467(E) (1987).
- [30] K. Huang and P. Tommasini, J. Res. Natl. Inst. Stand. Technol. **101**, 435 (1996).
- [31] Yu. N. Demkov and V. N. Ostrovskii, *Zero-range Potentials and their Applications in Atomic Physics* (Plenum, New York, 1988, translated from Russian by A. M. Ermolaev), see pp. 4–9.